

Mimicking Tissue Surfaces by Supported Membrane Coupled Ultrathin Layer of Hyaluronic Acid[†]

Kheya Sengupta,^{*,‡} Jörg Schilling,[‡] Stefanie Marx,[‡] Markus Fischer,[§]
Adelbert Bacher,[§] and Erich Sackmann[‡]

*Lehrstuhl für Biophysik, E22, Technische Universität München, James-Franck-Strasse 1,
D-85748 Garching, Germany, and Institut für Organische Chemie und Biochemie,
Technische Universität München, Lichtenbergstrasse 4, D-85748 Garching, Germany*

Received June 28, 2002. In Final Form: September 10, 2002

We describe a technique of anchoring ultrathin (50–250 nm) layers of the extracellular matrix polysaccharide hyaluronic acid (HA) on solid supported fluid lipid bilayers through a recombinant HA-binding protein (p32) which is coupled to lipid molecules by reversible histidine–chelator bonds. A novel technique, the dual wavelength reflection interference contrast microscopy (DW-RICM), was applied to measure the local absolute thickness of the soft polymer cushions by measuring the height of the colloidal beads hovering over the surface. By analysis of the mean-square out-of-plane fluctuations of the beads, the surface elasticity and friction of the HA films can be measured as a function of the film thickness. The technique is applied to study the influence of excess salt and the cross-linkers on the film thickness and viscoelastic parameters of membrane coupled HA layer. The mean-square displacement of the lateral diffusion of the colloidal beads over the HA film obeys a non-Brownian power law $\langle |x(t) - x(0)|^2 \rangle \propto t^\alpha$ with $\alpha = 0.70 \pm 0.05$ attributed to the time-dependent friction of the viscoelastic HA film.

Introduction

Hyaluronic acid (HA, also called hyaluronan) is a linear anionic polysaccharide composed of disaccharide repeat units exhibiting one carboxyl group. It is a megadalton polyelectrolyte of up to 50 000 repeat units. At neutral (physiological) pH the carboxyl groups are dissociated resulting in high solubility of the polymer in water. Due to strong steric and electrostatic repulsion, hyaluronic acid swells strongly in water (up to 0.1 vol % HA per unit volume of water).¹

Hyaluronic acid is a multifunctional molecule which plays an important role as structural constituent of tissues. Moreover, it is attached through cell surface receptors (such as CD44) to migrating cells² and has been found more recently to also play an important role inside cells both for signal transduction and the processing of RNA during gene expression.³ The role of HA as an ubiquitous structural element, for instance in the vitreous humor of the eye ball or as lubricating fluid between joints, is due to the strong swelling behavior of the polyelectrolyte and the soft viscoelastic impedance of entangled polymers in solutions. Depending on the presence of HA receptors (such as CD44) on the cell surface, the hyaluronic acid molecules may act as attractive or repulsive spacers between cells. HA can separate the cells in tissues by a few hundred nanometers, thus enabling their relative motion and preventing receptor-mediated cell aggregation. This property of HA is important during embryonic development such as the formation of skeletal muscles⁴ or of the neural tube.⁵

The present work is motivated by continuous efforts at our laboratory to design mimetics of cell and tissue surfaces on solid substrates by deposition of supported membranes, ultrathin polymer cushions, or supported membranes separated from the solid substrate by ultrathin polymer cushions.⁶ In a previous study we created HA polymer cushions on glass substrates by anchoring HA through covalent bonds on self-assembled aminosilane monolayers. The drawback of the procedure is that the density and the mobility of the HA-anchoring sites cannot be controlled and the average film thickness at physiological ionic strength (~ 150 mM) was rather small (≈ 60 nm).⁷

In the present work we developed a more bioanalogous system by anchoring HA films to solid supported membranes through the recombinant intracellular HA binding protein p32. The protein exhibits a histidine tail and can thus be specifically anchored to fluid-supported lipid bilayers through embedded chelating lipids;⁸ cf. Figure 1. The local film thickness and the surface viscoelastic moduli are measured by a previously developed colloidal probe technique based on the analysis of the out-of-plane Brownian motion of colloidal probes hovering over the film.^{7,9} The novel dual wave–interferometric technique (reflection interference contrast microscopy) enables the measurement of the absolute film thickness with 4 nm absolute resolution and thus allows the establishment of correlations between surface viscoelastic parameters and the film thickness.

* To whom correspondence may be addressed. E-mail: ksengupt@ph.tum.de.

[†] Part of the *Langmuir* special issue entitled The Biomolecular Interface.

[‡] Lehrstuhl für Biophysik.

[§] Institut für Organische Chemie und Biochemie.

(1) Hascall, V. C.; Laurent, T. C. Review article in: <http://www.glycoforum.gr.jp/science/hyaluronan/HA01/HA01E.html>.

(2) Zimmerman, E.; Geiger, B.; Addadi, L. *Biophys. J.* **2002**, *82*, 1848–1857.

(3) Lee, J. Y.; Spicer, A. P. *Curr. Opin. Cell Biol.* **2000**, *12*, 581–586.

(4) Lodish, H.; Baltimore, D.; Berk, A.; Zipursky, S. L.; Matsudaira, P.; Darnell, J. *Molecular Cell Biology*, 3rd ed.; Scientific American Books Inc.: New York, 1995.

(5) Toole, B. P. *Cell Biology of Extracellular Matrix*, 2nd ed.; Hay E. D., Ed.; Plenum Pub Corp.: New York, 1992.

(6) Tanaka, M.; Sackmann, E. *Trends Biotechnol.* **2000**, *18*, 57–64.

(7) Albersdörfer, A.; Sackmann, E. *Eur. Phys. J. B* **1999**, *10*, 663–672.

(8) Dorn, I.; Neumaier, K.; Tampé, R. *J. Am. Chem. Soc.* **1998**, *120*, 2753–2763.

(9) Kühner, M.; Sackmann, E. *Langmuir* **1996**, *12*, 4866–4876.

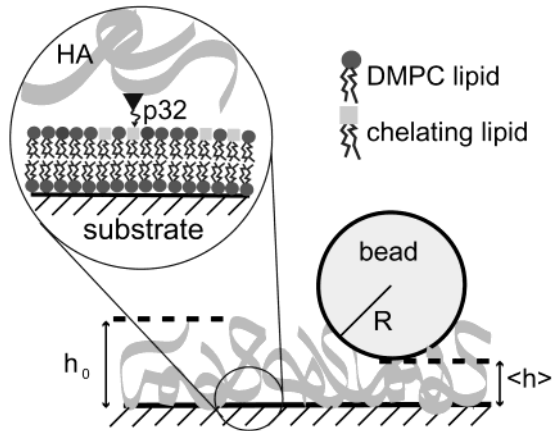


Figure 1. Schematic view of the supported hyaluronic acid (HA) film grafted to a membrane by HA binding protein p32-his6 with a colloidal bead hovering over the HA film. Note the drawing is not to scale.

Materials and Method

Hyaluronic Acid. Sodium salt of hyaluronic acid was purchased from Sigma-Aldrich, Chemie GmbH, Germany, and was used without further purification. The molecular weight of the polymer used is 1.24 MDa, which corresponds to 3100 disaccharide units or an end-to-end length of about 3 μm . Some of the HA was fluorescently labeled, and fluorescence microscopy was used to confirm that HA does not bind unspecifically to lipid monolayers but does bind to the membrane when the HA-binding protein p32 mediates the binding. However, all the RICM experiments were done using unlabeled HA.

Preparation of the HA Binding Protein P32. The hyaluronic acid binding protein p32 exhibiting a histidine tag was synthesized locally by genetic engineering. p32 is a trimer and has three hyaluronic acid binding sites.¹⁰ Also, as discussed earlier, the protein can bind to a nickel chelating lipid through the histidine tag.⁸ Therefore, p32 was used both to anchor the hyaluronic acid to the substrate and as cross-linkers. A detailed description of the preparation procedure is given in the Appendix.

Sample Preparation. Thoroughly cleaned glass cover slides were coated with lipid bilayers using Langmuir–Schaefer technique. The first (lower) monolayer consisted of pure DMPC (dimyristoleoyl phosphatidylcholine); all lipids were purchased from Avanti Polar Lipids Inc., AL. The second monolayer consisted of a mixture of DMPC and a lipid with a nickel chelating headgroup: Ni–NTA–DOGS (nitriloacetic acid dioleoyl-*sn*-glycero-3-[*N*-(5-amino-1-carboxypentyl)iminodiacetic acid)succinyl]). Both the monolayers were deposited at a surface pressure of 25–30 mN/m and a temperature of 25 $^{\circ}\text{C}$.

The bilayer-coated slide was immersed in a HEPES (4-(2-hydroxyethyl)piperazine-1-ethansulfonic acid, Sigma) buffer solution at pH = 7.2 and was transferred to a water-tight chamber of 1 mL volume. Ten micrograms of the receptor protein p32-his6 was introduced into this chamber. After about 30 min, the buffer was exchanged to remove any unbound p32 and 10 μL of a 0.1 mg/mL solution of hyaluronic acid was added. Again, after 30 min, the buffer was exchanged to remove excess hyaluronic acid. This completed the sample preparation.

To measure the effect of excess salt (KCl) or excess cross-linkers (p32) the initial thickness was first measured in the absence of salt and cross-linkers. Next, salt (or cross-linkers) was added. Sufficient time was allowed for

equilibrium to be established before the next measurement was performed. This allows us to compare the height and viscoelastic properties of each sample before and after the addition of salt or cross-linkers.

Preparation of the Beads. Polystyrene beads of 10 μm diameter were purchased from Polysciences, Inc., PA. Prior to an experiment, the beads were incubated at room temperature in a 3 wt % solution solution of bovine serum albumin (BSA, Sigma) for about 20 min and then washed thoroughly to remove excess BSA from the solution. The beads are thus covered with a strongly adsorbed film of BSA. This step is necessary since otherwise, as observed in our control experiments, the beads simply stick to the HA because of hydrophobic attraction.

Dual Wavelength RICM. Reflection interference contrast microscopy was used to determine the local height of colloidal beads placed on the HA layer. In this method, the concentric fringes formed by interference of light reflected from the interface of water and the colloidal bead and from the interface between the glass substrate and water are recorded. In the past, RICM patterns were analyzed by fitting the experimentally observed pattern with the theoretically calculated one with the bead height as an adjustable parameter.⁹ This provides correct values for the relative height of the bead with a resolution of ± 3 nm, but since the interference pattern is periodic with respect to the phase of the interfering light waves, it is not possible to determine the absolute height of the bead using the conventional RICM technique.

We have developed the dual wavelength RICM technique to overcome this limitation. In this technique, the bead is illuminated simultaneously with light of two different wavelengths and the pattern is recorded separately for each wavelength. By comparing the two patterns, it is possible to determine the absolute height of the bead. The detailed description will be published elsewhere.

Evaluation of the Elastic Potential and the Surface Viscosity of the Polymer Film. The Brownian motion of a colloidal bead in a potential $V(h)$ can be described by the Langevin equation

$$m \frac{\partial^2 h}{\partial t^2} + \gamma \frac{\partial h}{\partial t} + \frac{\partial V}{\partial h} = f_{\text{stoch}} \quad (1)$$

h is the distance of the bead from the substrate, m is the mass of the bead, t is the time variable, and f_{stoch} is the stochastic force due to thermal noise. In the case of a colloidal bead, the first term on the left-hand side, which is the inertial term, can be neglected. The second term accounts for the viscous force where γ is an effective friction coefficient. The third term accounts for the interfacial interaction potential $V(h)$ between the bead and the polymer film. Provided specific forces between the bead and the polymer are neglected, $V(h)$ is determined by the elastic restoring force of the polymer film. For small deformations $V(h)$ can be expressed in terms of a harmonic potential $V(h) = V''(\Delta h)^2$ where $V'' = \partial^2 V / \partial h^2$ and $\Delta h = h - \langle h \rangle$. V'' is a convenient measure of the surface elastic constant of the polymer film. Later on in this work V'' will be related to the Young modulus of the polymer film. The effective friction of a sphere exhibiting steady-state motion at a distance h from a wall is determined by a modified Stoke's law^{11,12}

$$\gamma = 6\pi R \eta_{\text{eff}} F\left(\frac{R}{h}\right) \quad (2)$$

where the function $F(R/h)$ accounts for the fluid drainage between the bead and the wall. However, this approach

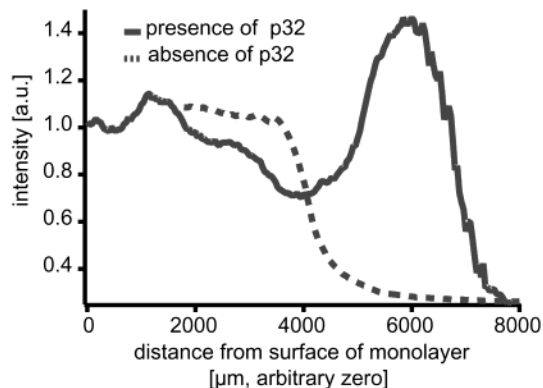


Figure 2. Distribution of fluorescence-labeled HA in the subphase of the film balance covered by a NTA-DOGS and DMPC–lipid film in absence (dashed line) and presence (drawn line) of p32-his6 determined by the z -scan technique.¹⁴

seems to be valid only for distances larger than 250 nm as we have learned from measurements of falling beads in buffer.¹³

The two viscoelastic parameters V'' and γ can be determined by measuring the time correlation function of the fluctuation of the distance between the bead and the planer solid surface according to

$$\langle h(t)h(t + \tau) \rangle = \frac{k_B T}{V''} \exp\left(-\frac{V''}{\gamma}\tau\right) \quad (3)$$

The second derivative of the interaction potential $V''(h)$ can also be obtained by measuring $V(h)$ through the distribution $P(h)$ of the mean square displacement $\langle |\delta x|^2 \rangle$ and by application of Boltzmann's law^{7,9}

$$V(h) = -k_B T \ln[P(h)/P_0] \quad (4)$$

We have confirmed that for our measurements the two methods yield approximately same value for $V''(h)$ (data not shown).

Results and Discussion

Test of the Functionality of p32. To check whether p32 does indeed anchor hyaluronic acid to membranes containing chelator lipids in a selective way, we studied the binding of fluorescently labeled HA to monolayers of DMPC containing 20% Ni–NTA–DOGS in the absence and presence of p32. The binding is tested by microfluorescence using the z -scan technique.¹⁴ The fluorescence intensity is recorded while the objective of the microscope is moved in the vertical (z) direction. Figure 2 shows the fluorescence intensity distributions with and without the anchor protein p32. While for the case where there is no p32 added, the fluorescence intensity decays monotonically when the focus of the objective is moved from the subphase to the air, a sharp peak arises in the presence of p32, demonstrating that p32 mediates specific binding of HA to lipid layers containing chelating lipids. The binding of p32 was also demonstrated by the surface plasmon resonance technique using a Biacore Instrument (Biacore Inc., NJ) (See Figure 3).

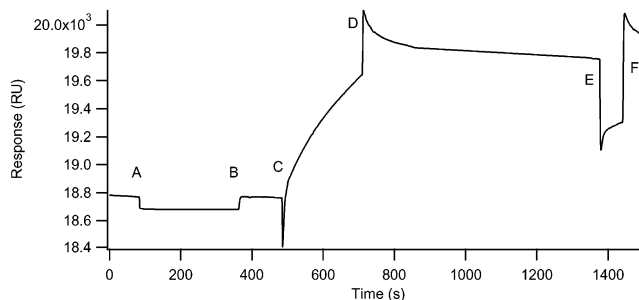


Figure 3. Plot of SPR-response signal showing binding of p32-his6 and HA to a NTA biacore chip covered with Ni-chelating groups. (A) Injection of HA directly on NTA surface. The slight decrease in response signal is attributed to the change in refractive index because of presence of HA in the buffer. (B) Washing the chip with buffer results in complete recovery of the original signal showing that HA does not absorb unspecifically to the chip. (C and D) Injection of p32-his6 followed by a washing step. A clear increase in the signal is observed indicating that the receptor had bound to the chip. (E and F) Injection of HA and subsequent washing. There is a net increase in the response signal indicating that HA binds to the p32-his6 covered surface.

Table 1. Summary of the Average Thickness $\langle h \rangle$, the Standard Deviation of the Thickness σ , and the Root-Mean-Square Amplitude of the Thermal Fluctuation of the Beads, Δh , for HA Films Deposited on Membrane with 20% and 1% Ni–NTA–Lipids^a

system	1% NTA			20% NTA		
	$\langle h \rangle$	σ	Δh	$\langle h \rangle$	σ	Δh
low salt, no p32	231	40	24	225	45	30
200 mM KCl, no p32	97	15	5	142	32	20
low salt, 10 μ g/mL p32	274	40	32	229	62	30

^a All heights are given in nm.

Thickness of HA Film in Low and High Salt Buffer.

We measured the thickness of HA films for different ionic strengths of the buffer and as a function of concentration of anchoring lipids in the top monolayer of supported membranes by doping DMPC with 1% and 20% chelating lipids. The data are summarized in Table 1 which shows measurements of the average film thickness $\langle h \rangle$, the standard deviation of the spatial variations of the thickness (σ), and the root-mean-square amplitude of the thermal fluctuation (Δh) of the beads.

The data in the third row hold for freshly deposited HA films in 5 mM (pH = 7.2) HEPES buffer (referred hereafter as the low salt buffer) averaged over two samples and 10 different lateral positions for each sample. We have checked (in the case of 20% anchoring chelating lipids) with over 15 samples that these results are reproducible. The data in the fourth row were obtained by changing the buffer to excess salt conditions (5 mM HEPES, 200 mM KCl, pH = 7.2) in one of the two samples whose average is reported in row three. The data presented in row five were obtained by adding excess cross-linkers to the second of the two samples whose averages are presented in the third row. For each of these, the data presented are averages over 16 different lateral positions on the sample. The reproducibility of the results with excess salt and cross-linker (for 20% chelating lipids) was checked for over 5 different samples in each case.

The measured thickness ($\langle h \rangle$) of the freshly deposited HA films is 225 nm. The thickness at different locations within the same sample varies by $\approx 25\%$. The average height varies by 15% from sample to sample. In agreement with previous studies of covalently grafted HA films,⁷ the film thickness is decreased drastically by a factor of 2

(11) Happel, J.; Brenner, H. *Low Reynolds number hydrodynamics*, 2nd ed.; Kluwer Academic Publishers: Dordrecht, The Netherlands, 1991.

(12) Gelbert, M.; Biesalski, M.; Rühle, J.; Johannsmann, D. *Langmuir* **2000**, *16*, 5774–5784.

(13) Schilling, J. Doctoral thesis, Technische Universität München, Germany, 2002.

(14) Demé, B.; Hess, D.; Trisl, M.; Lee, L.; Sackmann, E. *Eur. Phys. J. E* **2000**, *2*, 125–136.

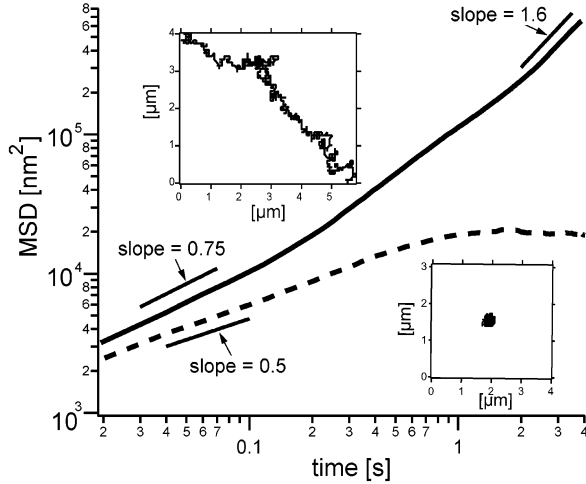


Figure 4. Characterization of local mobility of colloidal bead hovering over bare and HA-covered glass substrate in terms of the time dependence of in-plane mean square displacement of colloidal bead $\langle |r(t) - r(0)|^2 \rangle$. The insets show examples of typical random walks performed by the beads under different circumstances. The beads are locally trapped while hovering over bare glass whereas they can diffuse freely over HA films.

when excess salt (200 mM KCl) is added. The ion-induced condensation of the network is also associated with a remarkable decrease of the fluctuation amplitude of the beads hovering over the HA film.

Table 1 also shows that the HA film thickness does not depend appreciably on the lateral density of the chelating lipid anchor. This can be explained in terms of the large Flory radius of the polymer ($R_F \approx 120$ nm), which is large compared to the average distance between the anchor points at 1% anchoring lipid concentration (≈ 6 nm). The average film thickness agrees reasonably well with the Flory diameter meaning twice the Flory radius of the polymer in a good solvent: $R_F = aN^{3/5}$, where a is the length and N is the number of repeat units, respectively. For $a \approx 1$ nm and $N = 3000$, one finds $R_F \approx 120$ nm. This suggests that the surface-grafted film consists of a monolayer of swollen HA chains which are anchored to the surface at their naturally occurring points of contact.

To test whether the protein p32 can be used not only as linker for surface grafting but as a natural cross-linker, its effect on the film thickness was measured. As follows from row five of Table 1, in the absence of salt, the addition of p32 induces a small but appreciable increase in the layer thickness increases, in contrast to the expectation that the film should condense if the protein was effective as cross-linker. The most likely explanation for the increase in thickness is that the HA layer is swollen by the protein which implies a higher solubility of the protein in the polymer layer than in water.

Lateral Mobility. As a first test of the effect of the HA-layer on the dynamic behavior of the bead, we analyze the time dependence of the mean-square displacement $\langle \Delta x(t) \rangle^2 = \langle |x(t) - x(0)|^2 \rangle$ of the lateral motion of the bead hovering over bare and HA-covered glass. This test enables simultaneous exclusion of artifact due to directed local flow induced by thermal convection. Figure 4 shows a remarkable difference in the behavior of $\langle \Delta x(t) \rangle$ between the two surfaces.

Over bare glass the beads perform a restricted Brownian motion since the root-mean-square amplitude scales as $\langle \Delta x(t) \rangle \propto t^{1/2}$ at small times but saturates at longer times. This behavior suggests that the beads tend to stick locally to the bare glass surface. The beads hovering over the HA film exhibit nonrestricted random walks, and the root-

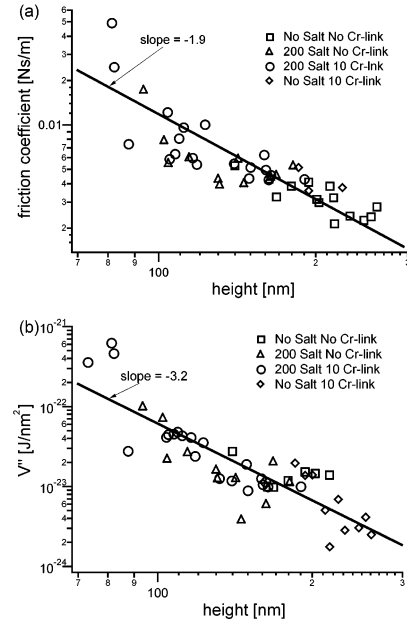


Figure 5. (a) Plot of second derivative of the interaction potential V'' (force constant characterizing resistance of HA layer against elastic deformation) as function of absolute local thickness of HA layer. Data are obtained under three different conditions: (1) low ionic strength; (2) high ionic strength $c_1 = 200$ mM KCl; (3) low ionic strength in the presence of $10 \mu\text{M}$ cross-linker p32; (4) high ionic strength $c_1 = 200$ mM KCl in the presence of $10 \mu\text{M}$ cross-linker p32. The drawn line corresponds to an optimal fit of the monotonic increase of V'' with decreasing layer thickness by a power law $V'' \sim h^{-3.2}$.

mean-square displacement obeys an approximate scaling law $\langle \Delta x(t) \rangle \propto t^{3/4}$ associated with the frictional coupling to the polymer film.

Analysis of Viscoelastic Parameters. In Figure 5a we present measurements of the second derivative of the interfacial potential V'' as a function of the height h of the bead above the solid surface. To compare a large range of distances, we summarize the measurements obtained under the following conditions in one graph: (a) at low ionic strength of the aqueous phase (5 mM HEPES); (b) at high ionic strength (200 mM KCl); (c) at low ionic strength but in the presence of excess cross-linkers p32; (d) at high ionic strength and in the presence of excess cross-linker p32 ($0.3 \mu\text{M}$) in the aqueous phase. The data clearly show a monotonic increase of the force constant $k = V''$ (that characterizes the effective elastic stiffness of the polymer film) with decreasing layer thickness. The behavior can be characterized by an empirical power law $V'' = d^{\alpha \pm \delta \alpha}$ with $\alpha = -3.2$ and $\delta \alpha = 0.3$ (solid line in Figure 5a). The effective surface friction coefficient γ can be determined from the relaxation time of the time correlation function defined in eq 3. The values are summarized in Figure 5b. Similar to the behavior of V'' the friction increases monotonically with decreasing film thickness.

The mean square displacement (MSD) analysis of the tangential random motion of a bead hovering over bare glass surfaces shows the typical features of a harmonic potential (dashed line in Figure 4), whereas the MSD for a bead on the polymer film clearly demonstrates the interaction of the bead with polymer since the MSD scales with time approximately as $\langle |x(t) - x(0)|^2 \rangle \propto t^{3/4}$ (drawn line in Figure 4). The superdiffusive motion is a consequence of the fact that the frictional coefficient of the polymer film is time dependent $\gamma_s(t)$. The thermally driven MSD obeys the general equation $(d/dt)\langle |x(t) - x(0)|^2 \rangle =$

$4(k_B T/\gamma_s(t))$, and in agreement with our experimental results $\gamma_s(t)$ scales as $\gamma_s(t) \propto t^{1/4}$.¹⁵

For practical applications it is useful to relate the surface viscoelastic moduli V'' and γ to the bulk elastic modulus (Young modulus E) and viscosities of the films. To achieve this we first apply the modified Stokes law (eq 2 with $F(R/h) = R/h$) and the Hertz model as modified by Johnson, Kendall, and Roberts (HJKR model¹⁶). Consider first the viscosity. The Stokes model is expected to be valid for thicknesses of the order of $\langle h_0 \rangle \geq 250$ nm as follows from separate studies of the colloidal bead motion over bare glass substrates.¹³ Thus we find a viscosity $\eta_{\text{H}_2\text{O}} \sim 2$ mPa s, which is a factor of 2 larger than the bulk water viscosity. The value for the HA film for $\langle h_0 \rangle \sim 250$ nm is of the same order $\eta(\text{HA}) \sim 2$ mPa s.

Consider now the elastic behavior. Due to the gravitational force the bead will create an indentation of depth $\delta h = h_0 - \langle h \rangle$, and the measured average film thickness $\langle h \rangle$ is thus smaller than the thickness of the unperturbed HA film $\langle h_0 \rangle$. Since the mass density of the colloidal bead ($\rho = 1.07 \times 10^3$ kg/m³) is comparable to that of water ($\rho = 1.0 \times 10^3$ kg/m³), the indentation is small compared to the film thickness. We therefore assume that the Hertz model is a good approximation to account for the deformation of the polymer film by the colloidal probe. This allows us, in a first approximation, to relate the Young modulus E to the force constant V'' defined by the Langevin equation (eq 1) by equating the deformation energies.

Assuming that the HA film is incompressible (Poisson ratio = $1/2$), the deformation energy predicted by the Hertz model is (ref 17, section 9)

$$U_{\text{ela}}^{\text{Hertz}} = \frac{32}{45} \frac{E}{R^{1/2}} (\delta h)^{5/2} \quad (5)$$

and for the Langevin (eq 1) model it is

$$U_{\text{ela}}^{\text{Langevin}} = \frac{1}{2} V'' (\delta h)^2 \quad (6)$$

Equating the two energies yields

$$E = \frac{45}{64} \frac{V''}{R^{1/2}} (\delta h)^{-1/2} \quad (7)$$

Now, δh can be obtained from eq 9.14 in ref 17¹⁷

$$\delta h = \left(\frac{9}{16} \right)^{2/3} E^{-2/3} R^{-1/3} F_g^{2/3} \quad (8)$$

Since the gravitational force F_g is known, the Young modulus can be determined from V'' according to

$$E \approx 0.79 R^{-1/2} F_g^{-1/2} (V'')^{3/2} \quad (9)$$

With the value of E known, the depth of the indentation is obtained from the Hertz model (eq 8).

The density difference between the polystyrene and H₂O is $\delta\rho \approx 0.7 \times 10^3$ kg/m³, and thus $F_g \approx 0.4 \pm 0.1$ pN. For the case $\langle h_0 \rangle \approx 250$ nm and $V'' \approx 10^{-3}$ k_BT/nm², one obtains $E = 4 \pm 1$ Pa and $\delta h \approx 100$ nm. For the case $\langle h_0 \rangle \approx 100$ nm at 200 mM KCl, one estimates $E = 100$ –300 Pa and $\delta h = 5$ –10 nm. The value of $E \approx 200$ Pa agrees

(15) Caspi, A.; Granek, R.; Elbaum, M. *Phys. Rev. Lett.* **2000**, *85*, 5655–5658.

(16) Johnson, K. L.; Kendall, K.; Roberts, A. D. *Proc. R. Soc. London* **1971**, *324*, 301–313.

(17) Landau, L. D.; Lifshitz, E. M. *Theory of Elasticity*, 3rd ed.; Pergamon Press Inc.: New York, 1986.

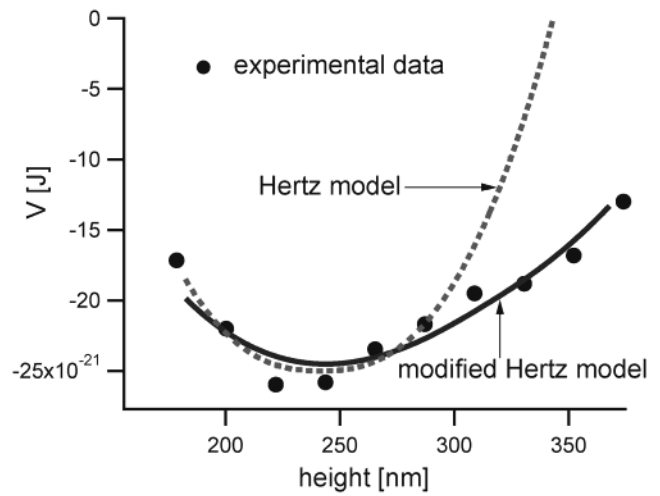


Figure 6. The data determining the interaction potential $V(h)$ are obtained from the probability distribution of the height of a bead over the HA film as calculated by the Boltzmann law (eq 4). The dashed line is the best fit to the data following the Hertz model (eq 5), and the drawn line is the best fit to the HJKR model (eq 10).

well with measurements of the Young modulus of thick slightly cross-linked HA layers yielding $E = 3$ –300 Pa depending on the degree of cross-linking.¹⁸

The Hertz model ignores the specific interaction between the bead and the substrate. This is accounted for in the HJKR model,¹⁶ which yields for the total interaction potential

$$V(h) = \frac{32}{45} ER^3 \left(\frac{\delta h}{R} \right)^{5/2} - \pi W_{\text{ad}} R(\delta h) + \frac{4\pi}{3} (\Delta\rho) g R^3 \langle h \rangle + C \quad (10)$$

where W_{ad} is the specific adhesion energy and $\Delta\rho$ is the density difference between the polystyrene bead and the buffer. The gravitational potential is known, and as described above the interaction potential can be determined from the distribution of height fluctuations by Boltzmann's law following Albertsdörfer et al.⁷ By fitting eq 10 to the measured potential, one can thus also determine the Young modulus E and the adhesion energy W_{ad} and by considering the known value of the gravitational force. The data of Figure 6 have been analyzed in this way. For the case of the HA layer of 250 nm thickness one finds $E \approx 10$ Pa, $\delta h \approx 50$ nm, and $W_{\text{ad}} \approx 1 \times 10^{-8}$ J/m². The values of E and δh agree well with the values determined by the direct analysis in terms of the Hertz model given above. The interaction energy W_{ad} agrees astonishing well with the van der Waals attraction (W_{vdw}) between two planar condensed surfaces at a distance h : $W_{\text{vdw}} = -A/12\pi h^2$. For polystyrene–water–glass interface $A \approx 1 \times 10^{-20}$ J and at $d \approx 200$ nm, one obtains $W_{\text{vdw}} = 10^{-8}$ J/m².

Concluding Discussions

We developed a versatile method to generate bioanalogous soft polymer cushions on solid supports with thicknesses in the 100 nm range. The anchoring sites can be made mobile by grafting the polysaccharides to fluid-supported membranes. Therefore, the designed system could also serve as a model for cell surfaces that exhibit

(18) Ladam, G.; Vonna, L.; Sackmann, E. Unpublished results.

Table 2. Bacterial Strains and Plasmids

strain or plasmid	relevant characteristics	source
<i>E. coli</i> strains:		
XL-1-Blue	recA1, endA1, gyrA96, thi-1, hsdR17, supE44, relA1, lac[F, proAB, lacI ^q ZΔM15, Tn10(tet ^r)]	ref 24
M15 [pREP4]	lac, ara, gal, mtl, recA ⁺ , uvr ⁺ , [pREP4: lacI, kan ^r]	a
Plasmids:		
pNCO-SB-His6-ACYC184	high copy His-tag expression vector	ref 23
pNCO-HS-P32-Streptag	vector expressing HS-P32-Streptag	b

^a Zamenhof, P. J.; Villarejo, M. *J. Bacteriol.* **1972**, *110*, 171–178. ^b This study.

Table 3. Oligonucleotides Used for Construction of RIB5 Expression Plasmid

designation	endonuclease	strand	sequence (5' to 3')
HSP32-Rbs-EcoRI	EcoRI, NcoI	forward	ataatagaattcattaagaggagaaattaacatggg-tcacaccgacggag
HSP32-HindIII-Hi	HindIII	reverse	tattattataagcttactgctcttgacaaaactcttgag

hyaluronic acid layers attached to cell surfaces through receptors such as CD44.⁵ One main motivation for the present efforts was to generate biocompatible surfaces for stress-free immobilization of cells for studying the physical basis of cell adhesion.¹⁹ In separate experiments with several 100 μm thick chemically anchored and cross-linked HA layers on solids, it was found that cells of the slime mold *Dictyostelium discoideum* adhere on HA films while mammalian cells such as fibroblasts do not. However, the latter type of cells adheres to HA layers decorated with random arrays of polystyrene beads and covered with fibronectin.¹⁸

By combining the dual wavelength interferometry and the colloidal bead motion analysis, it is possible to characterize the viscoelastic properties of the polymer films in terms of the surface viscosity and surface elasticity as a function of the film thickness. Such measurements are essential for future applications of supported HA films for quantitative studies of cell locomotion and cell adhesion since both processes depend critically on the elasticity of the substrates. The correlation between cell locomotion and the elasticity of the substrate was established in several studies.^{2,20,21} In these cases the substrates consisted of polymer films of several hundred micrometer thickness exhibiting elasticities of the order of several hundred pascals. Using HA, it would be possible to extend such measurements to much softer and thinner substrates which can mimic situations encountered during embryo development.⁵

The microinterferometric technique used in the present work is limited to soft films since the spatial resolution of the relative height measurement is about 1 nm. Higher resolutions can be obtained with the atomic force microscopy (AFM) technique using AFM tips with attached colloidal beads.¹² However, this method is limited to measurements of spring constants V'' of the order of several newtons per meter. The two methods are thus complementary.

Our attempts to control the elasticity of the HA layers through the natural cross-linker p32 have not been successful yet, which could be due to the fact that the protein can bind only to chain ends of the polysaccharides. However, HA can be cross-linked covalently through amines and the elasticity can be controlled by this method of cross-linking.¹⁸

Acknowledgment. We thank Dr. M. Bärmann and G. Chmel for the preparation of the fluorescent-labeled HA, M. Rusp for electron microscopy of the polystyrene beads, and Dr. E. Sinner for the use of a Biacore SPR instrument. The present work was supported by the Deutsche Forschungs Gesellschaft (SFB 563, project C5), the Fonds der Chemischen Industrie. The work was also supported partially by the USA National Science Foundation ITP PHY/99-0749. K.S. thanks the Humboldt Foundation for a research fellowship.

Appendix. Preparation of p32

Materials. Oligonucleotides were custom synthesized by Interactiva, Ulm, Germany. Restriction enzymes were from New England Biolabs, Schwalbach, Germany. T4-DNA ligase and reverse transcriptase (SuperScriptII) were from Gibco BRL, Eggenstein, Germany. Taq-Polymerase was from Finnzyme, Espoo, Finland. DNA fragments were purified with the QIAquick PCR Purification Kit from Qiagen, Hilden, Germany.

Microorganisms and Plasmids. Microorganisms and plasmids used in this study are summarized in Table 2.

Preparation of cDNA. The human cDNA (encoding HS-P32) was obtained from human adult liver PolyA⁺ RNA (Stratagene, La Jolla, CA). The preparation of cDNA was performed as described earlier.²²

Construction of a His6–HS–P32 Expression Plasmid. The coding region (accession number T40995) representing the mature P32 was amplified by PCR using human liver cDNA as template and the oligonucleotides HSP32-Rbs-EcoRI and HSP32-HindIII-Hi as primers (cf. Table 3). The amplicate was digested with Eco RI and Hind III and was ligated into the expression vector pNCO-SB-His6-ACYC184,²³ which had been digested with the same enzymes yielding the plasmid designated pNCO-His6-HS-P32.

Transformation of *E. coli* Cells. *E. coli* XL-1 Blue cells were transformed with ligation mixtures by established procedures.²⁴ Transformants were selected on LB agar plates supplemented with ampicillin (170 mg/L). All plasmid constructs were sequenced by the automated dideoxynucleotide method²⁵ using a 377 Prism DNA

(19) Sackmann, E.; Bruinsma, R. *ChemPhysChem* **2002**, *3*, 262–269.

(20) Munerar, S.; Wang, Y.; Dembo, M. *Biophys J.* **2001**, *80*, 1744–1757.

(21) Balaban, N. Q.; Schwarz, U. S.; Riveline, D.; Goichberg, P.; Tzur, G.; Sabanay, I.; Mahalu, D.; Safran, S.; Bershadsky, A.; Addadi, L.; Geiger, B. *Nat. Cell Biol.* **2001**, *3*, 466–472.

(22) Fischer, M.; Haase, I.; Feicht, R.; Richter, G.; Gerhardt, S.; Changeux, J. P.; Huber, R.; Bacher, A. *Eur. J. Biochem.* **2002**, *269*, 519–26.

(23) Rohdich, F.; Wungsitaweekul, J.; Lüttgen, H.; Fischer, M.; Eisenreich, W.; Schuhr, C. A.; Fellermeier, M.; Schramek, N.; Zenk, M. H.; Bacher, A. *Proc. Natl. Acad. Sci. U.S.A.* **2000**, *97*, 8251–8256.

(24) Bullock, W. O.; Fernandez, J. M.; Short, J. M. *BioTechniques* **1987**, *5*, 376–379.

(25) Sanger, F.; Nilen, S.; Coulson, A. R. *Proc. Natl. Acad. Sci. U.S.A.* **1977**, *74*, 5463–5467.

sequencer from Applied Biosystems (Weiterstadt, Germany). The expression plasmids reisolated from XL-1 Blue cells were transformed into *E. coli* M15 [pREP4] cells carrying the pREP4 repressor plasmid for the over-expression of lac repressor protein. Kanamycin (15 mg/L) and ampicillin (170 mg/L) were added to secure the maintenance of both plasmids in the host strain. In the pNCO113 expression plasmids, the HS-P32 variants are under control of the T5 promoter and the lac operator.

Protein Purification. Recombinant *E. coli* strains were grown in LB medium containing ampicillin (150 mg/L) at 37 °C. At an optical density (600 nm) of about 0.7–0.9, isopropylthiogalactoside was added to a final concentration of 2 mM. After incubation for 5 h, the cells were harvested by centrifugation (Sorvall GS3 rotor, 5000 rpm, 15 min, 4 °C), washed twice with 0.9% NaCl, and stored at –20 °C. The frozen cell mass was thawed in

buffer A containing 100 mM Tris-hydrochloride, pH 8.0, containing 0.5 M sodium chloride and 0.02% sodium azide. The suspension was cooled on ice, ultrasonically treated and centrifuged (Sorvall SS34 rotor, 15000 rpm, 15 min, 4 °C). The supernatant was applied to a column of Ni-chelating Sepharose FF (2.6 × 5 cm, Amersham Pharmacia) previously equilibrated with buffer A. The column was washed with 150 mL of the buffer and was developed with a linear gradient of 20–500 mM imidazole hydrochloride in 130 mL of the buffer (flow rate, 3 mL min⁻¹). Fractions were combined and concentrated and applied to a Superdex 200 column (2.6 × 60 cm), which had been equilibrated with buffer A (flow rate, 3 mL min⁻¹). Fractions were again combined and concentrated by ultrafiltration.

LA0261460